ChemPubSoc Europe

DOI: 10.1002/cphc.201700439

CHEMPHYSCHEM Articles

Self-Assembly and Local Manipulation of Au-Pyridyl Coordination Networks on Metal Surfaces

Yang Song,[a] Yuxu Wang,[a] Qiao Jin,[b] Kun Zhou,[a] Ziliang Shi,*[a] Pei-Nian Liu,*[b] and Yu-qiang Ma*[a, c]

Using scanning tunnelling microscopy (STM), we demonstrate that Au-pyridyl coordination can be used to assemble two-dimensional coordination network structures on metal surfaces. The polymorphism of the coordination network structures can be manipulated at both the micro- and nanoscale. Using the same organic ligand, we assembled two distinct polymorphic network structures, which were assisted by threefold Au-pyridyl coordination on Ag(111) with predeposited Au atoms (α-network), and by twofold Au-pyridyl coordination on Au(111) (β-network), respectively. Specifically on the Au(111) surface, single-oriented β-network domains as large as ≈400 nm were selected by thermal annealing. We ascribe this global control strategy to distinct Au bonding modes tuned by molecule–substrate interactions. Using an STM tip, we succeeded in creating α-network domains (≈10 nm) locally within the homogeneous β-network domain areas on Au(111) in a controlled manner.

1. Introduction

Supramolecular self-assembly on metal surfaces has been extensively investigated because the resulting nanostructures show potential for heterogeneous catalysis, gas storage and magnetic storage.[1–11] The distinct physical/chemical properties of these low-dimensional nanostructures originate from both the characteristics of organic ligands and/or metal ions/atoms, that constitute the building blocks of a self-assembly, and particularly how these building blocks are interacted and thus arranged on a solid substrate. Therefore, it is essential to control the polymorphism of these supramolecular assemblies at both the micro- and nanoscale, aiming at tailoring and optimizing their functionality. Surface structures at different scales can be manipulated using various external stimuli, such as light, pH, and temperature.[12–19] For instance, Cometto et al. caused local conformational switching in a supramolecular network by polarizing the surface molecules using the tip of a scanning tunnelling microscope (STM).[18] Reversible manipulation at both the nano- and microscale in a supramolecular network were realized and used to control guest release and capture.[15,16]

Polymorphic network structures involving metal-organic coordination motifs have attracted particular interests because the ligands, bonding configurations and coordination numbers at the metal coordination centres can be judiciously modified, allowing to customize the catalytic and magnetic/spintronic characteristics. Coordination motifs also offer high thermal stability attractive for practical applications. Metal-organic frameworks have demonstrated potential in applications of light-emitting, sensing and optical/electronic nanodevices.[20–22] Regarding to these distinct properties of the coordination motif, researchers have made substantial efforts to control metal-organic coordination self-assembly on metal surfaces, such as by altering the type and concentration of organic ligands or metallic atoms (e.g. transition, alkali and lanthanide metals),[23–33] by selecting substrates and by tuning the ratio of metal/organic reactants.[6,23,30] Nevertheless, because of the intermediate of substrates and the liability of coordination motifs, controlling coordination assembly, especially at nanoscale, remains a challenge.

Here we demonstrate the self-assembly based on Au-pyridyl (py) coordination motifs, and the control over the polymorphism of the resultant two-dimensional coordination networks at both global and local scale. Two distinct polymorphic network structures were separately assembled by coordinating Au atoms with the same organic ligand 1,3,5-tris[4-(pyridin-4-yl)-phenyl]benzene **L** (Figure 1a, inset). One structure, named α-network, was formed via three-fold Au-py coordination on Ag(111) with predeposited Au atoms; the other structure, named β-network, was formed via two-fold Au-py coordination on Au(111). Thermal annealing of the network on Au(111) se-

[a] *Y. Song, Y. Wang, K. Zhou, Dr. Z. Shi, Prof. Y.-q. Ma*
Center for Soft Condensed Matter Physics & Interdisciplinary Research
College of Physics, Optoelectronics and Energy
Soochow University, 215006 Suzhou (China)
E-mail: phzshi@suda.edu.cn

[b] *Q. Jin, Prof. P.-N. Liu*
Shanghai Key Laboratory of Functional Materials Chemistry
Key Lab for Advanced Materials and
School of Chemistry & Molecular Engineering
East China University of Science and Technology
130 Meilong Road, Shanghai, 200237 (China)
E-mail: liupn@ecust.edu.cn

[c] *Prof. Y.-q. Ma*
National Laboratory of Solid State Microstructures and
Department of Physics, Nanjing University
Nanjing 210093 (China)
E-mail: myqiang@nju.edu.cn

The ORCID identification number(s) for the author(s) of this article can be found under https://doi.org/10.1002/cphc.201700439.

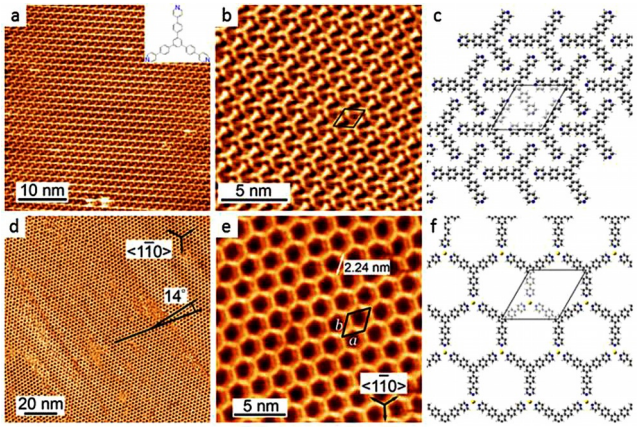

Figure 1. a) STM overview of the close-packed monolayer structure of organic ligand **L** (1,3,5-tris[4-(pyridin-4-yl)phenyl]benzene) on Ag(111). Inset: chemical structure of **L.** b) High-resolution image of the **L** monolayer. c) Tentative structural model of an **L** monolayer. d) STM overview of the Au-py coordination α-networks on Ag(111). Two domains oriented ≈14° relative to each other are visible. e) High-resolution image of the α-network. f) Tentative structural model of the α-network. The black rhombic frames in (b, c) and (e, f) delineate unit cells of, respectively, close-packed monolayers and α-networks. Colours in (c, f): C = grey; N = blue; H = white; Au = yellow.

lected exclusively single-oriented β-network domains as large as ≈400 nm. This global control appeared to depend on the liability of the Au-py coordination and a balance between metal-organic coordination and the molecule-substrate interactions. We were further able to locally manipulate the network structure by using an STM tip to create α-network domains (≈10 nm) locally within otherwise homogeneous β-network domains on Au(111).

2. Results and Discussion

First we examined whether Au (ad)atoms could coordinate with py with sufficient lability so that we could globally control the polymorphism of the resulting coordination networks through a choice of substrates or thermodynamic conditions.

2.1. Pure α-Network Phase on Ag(111)

Deposition of compound **L** onto a pristine Ag(111) surface at room temperature led to a close-packed monolayer structure in which each **L** molecule was in the same orientation and had six surrounding neighbours (Figure 1 a). The distance between neighbouring molecules was 1.58 ± 0.02 nm (Figure 1 b). We propose a tentative structural model based on high-resolution images (Figure 1 c). Based on the dimensions of **L** molecules in gas phase in which the distance between the two outermost N atoms was 1.74 nm, we deduced that the distance between the outermost N atoms of one molecule with the nearest H atoms in the central benzene of the neighbour molecule is 2.8–3.2 Å. This value falls within the typical distance range for H-bonds.[2] We annealed the sample up to 410 K in order to increase the density of Ag lattice-gas adatoms and promote mobility of the molecules.[34] Examination of the sample at room temperature showed that the thermal annealing did not alter the assembled close-packed structure. The formation of the close-packed structure under these conditions indicates an intermolecular N···H bonding that stabilizes **L** molecules, and excludes the possibility of Ag adatoms incorporation as coordination metal centres to py endgroups.

Consecutive deposition of Au atoms and **L** molecules on Ag(111), followed by thermal annealing at 390–450 K, generated a porous rhombic α-network structure (Figure 1 d). We defined the orientation of the α-network as one of three equivalent directions, along which two adjacent pores are aligned. Three rotational domains differing by 14 ± 2° were distinguished, one of which aligned with the $<1\bar{1}0>$ direction on the Ag(111) surface. **L** molecules in each domain were held together via py endgroups interlinked in a three-fold head-to-head manner (Figure 1 e). The unit cell (black rhombic frame in Figure 1 e) of the structure were defined by its two vectors (***a*** and ***b***) separated by 60°, and $|\boldsymbol{a}| = |\boldsymbol{b}| = 2.24 \pm 0.02$ nm.

We observed the α-network only when Au atoms were predeposited on the surface. This leads us to propose that Au atoms are incorporated into the intermolecular links, forming Au-py coordination that stabilizes the α-network. In a tentative model (Figure 1 f), we propose that each Au atom serves as a coordination centre to link three py endgroups, generating a rhombic lattice with a Au–N bond length of 2.7 Å.[35,36] Commensuration of surface coordination networks with the substrate is largely determined by molecule-substrate and/or metal centre–substrate interactions.[6,37] In the α-networks described here, the deviation of ±14° between the network orientation and the $<1\bar{1}0>$ direction indicates that the phenyl/py moieties of the adsorbed molecules coincide with none of high-symmetry sites on the substrate. This suggests a weak interaction between phenyl/py rings and the Ag(111) substrate, implying that adsorption of the Au coordination centres determines network orientation.

These experiments show that Au adatoms can serve as coordination centres in Au-py motifs. A three-fold configuration for surface-confined Au-py coordination is probably thermodynamically favoured, since the α-network in our experiments was maintained against thermal annealing up to 450 K.

2.2. Pure β-Network Phase and Single-Crystalline β-Networks on Au(111)

In contrast to what we observed on Ag(111), deposition of **L** molecules on a pristine Au(111) surface at room temperature led to a honeycomb β-network structure covering most of the surface (Figure 2 a). A small portion of the surface was covered by an α-network structure similar to that obtained on Ag(111) (see next section). The β-network structure showed two rotational domains separated by 30°, named β1- and β2-networks (Figure 2 a). High-resolution imaging revealed that the **L** molecules were held together via their py endgroups interlinked linearly in a head-to-head manner (Figure 2 b,c). Given the well-known repulsion between two pyridines, we propose that the Au atoms are incorporated into the links, forming two-fold Au-py coordination. Unit cell analysis indicated that the vector $\boldsymbol{a}_1$ in the β1-network was parallel to $<11\bar{2}>$ of the Au(111) sub-

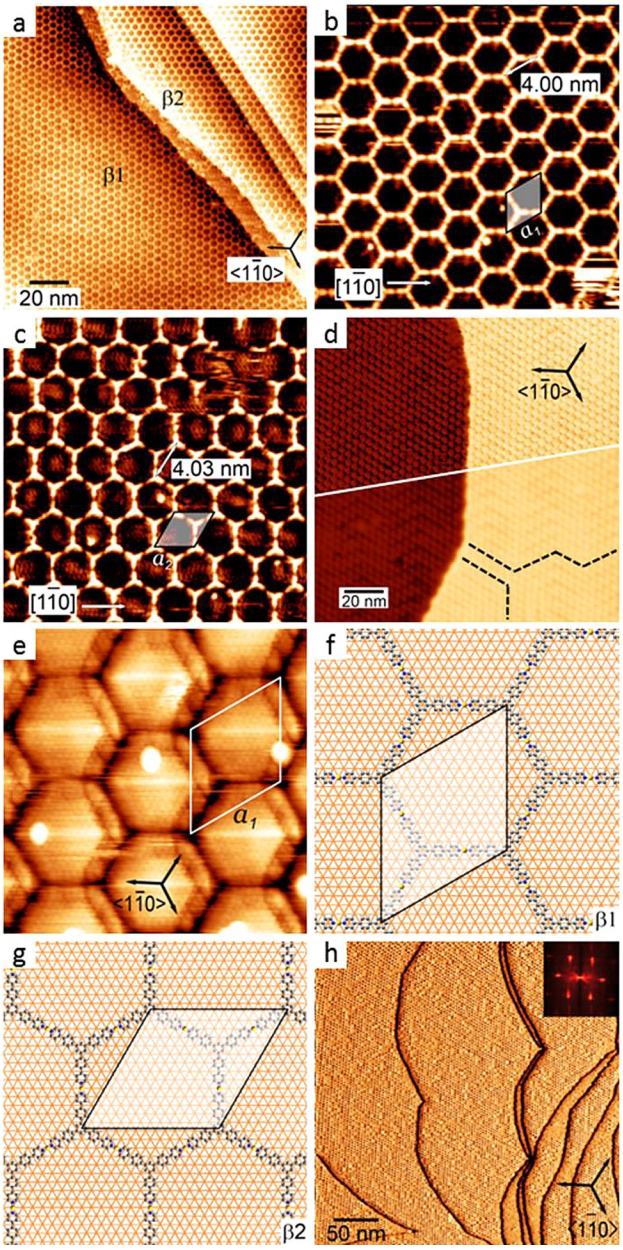

Figure 2. a) STM topograph of Au-py coordination β-networks out of deposition of molecule **L** on pristine Au(111). The domains β1 and β2 aligned along the $<11\bar{2}>$ and $<1\bar{1}0>$ vectors of the Au(111) substrate, respectively. b, c) High-resolution image of β1- and β2-networks. The unit cells are delineated as black rhombic frames ($|\boldsymbol{a}_1| = 4.00 \pm 0.02$ nm; $|\boldsymbol{a}_2| = 4.03 \pm 0.02$ nm). d) STM image show both β-networks (upper panel) and the underneath herringbone patterns (bottom panel). The bottom panel is artificially blurred to illustrate the herringbone patterns, two of them marked by zigzag dashed lines. e) STM topograph obtained with an atypical tip showing both the Au(111) atomic lattice and the β1-network. f, g) Tentative structural models of the β1- and β2-network with the underlying Au(111) lattice. Substrate Au atoms that serve as coordination centres are highlighted by yellow dots. h) Mapping of the tunnelling current in a typical STM analysis of a sample following a post-annealing at 540 K for 30 min. Inset in (h): FFT of the image.

strate, while the vector $\boldsymbol{a}_2$ in the β2-network was parallel to $<1\bar{1}0>$. The length of $\boldsymbol{a}_1$ and $\boldsymbol{a}_2$ were 4.00 ± 0.02 nm and 4.03 ± 0.02 nm, respectively. This suggests that the projected length of Au–N bond was 1.5 ± 0.1 Å in the β1-network and 1.6 ± 0.1 Å in the β2-network.

Au coordination on a Au(111) surface can occur when there exist Au adatoms lifted up from the substrate, in which case the Au(111) herringbone structure is usually "damaged".[38] Alternatively, the coordination centre can form when Au atoms at the "top" sites are slightly displaced; in this case, the Au(111) herringbone structure is preserved beneath the coordination structures.[39] By artificially blurring a typical STM image displaying a Au(111) surface area covered by β-networks (Figure 2d), we were able to observe integral herringbone patterns underneath the β-network. This indicates that the observed two-fold Au coordination centres are built via vertical displacement of substrate Au atoms. Consistently, Au coordination centres in β-networks coordinated with more substrate atoms and therefore fewer py endgroups than the three-fold Au-py coordination centres on Ag(111). It should be noted that in both α- and β-networks the Au coordination nodes (Figures 1e, 2b,c) showed similar depressed feature, which can be presumably attributed to a shorter Au coordination-surface distance with respect to the molecule-surface distance. Due to limitation of the instrument, we cannot determine unambiguously the height difference between two types of nodes.

Atomic-resolution imaging of the β1-network (Figure 2e) revealed the network to be commensurate with the substrate lattice, displaying an $(8\sqrt{3}\times 8\sqrt{3})R30^\circ$ superstructure. (The sites where the molecular centre adsorbed to the substrate could not be unambiguously determined because of a tip artefact.) We propose a tentative model of the β1-network on the Au(111) lattice (Figure 2f). In this model, Au atoms at the "top" sites serve as coordination metal centres (yellow dots in Figure 2f), and each of them coordinates with two N terminals belonging, respectively to two adjacent py endgroups. The resulting β1-network model is exactly commensurate with the Au(111) lattice; the deduced lattice constant of 3.99 nm indicates a Au-N coordination bond of 1.5 Å. We propose an analogue model for the β2-network, with the Au atoms at top sites acting as coordination centres (Figure 2g). The result is a commensuration superstructure (14×14) with a lattice constant of 4.03 nm, indicating a Au–N bond length of 1.6 Å. These lattice parameters for the β1- and β2-networks are in good agreement with STM observations. The quite small difference in the Au–N bond length for the two types of β-network implies a small bonding energy difference, presumably explaining why we observed the two oriented β-networks coexisting at room temperature.

The β-network covered most of the surface areas even after thermal annealing at high temperatures or for long durations, suggesting that the β-network is thermodynamically favoured on Au(111) in comparison with the α-network on Ag(111). Figure 2h shows a typical overview, represented by the mapping of the tunnelling current, of the sample resulted from a post-annealing at 540 K for 30 min, which manifests large single-orientated β1-network domains covering over several terraces. In fact, fast Fourier transform (FFT) of the image (Figure 2h, inset) showed clear discrete diffraction spots, indicating that all terraces were covered by β1-network. The single-crystalline domain

of the β1-network extended as long as 400 nm over an entire terrace.

Similar pure network phases on Ag(111) have been reported in which molecular adsorption onto the substrate induced formation of single-crystalline Co-sexiphenyl networks.[40] In our experiments, besides the small bonding energy difference due to the different Au–N bond lengths, the adsorption energy of the **L** molecule can also contribute to the emergence of the pure β1-network. For instance, a close inspection to the models reveals that the adsorption sites of the py or phenyl moieties for two network structures are considerably different. Future calculations based on density functional theory or experiments based on infrared reflection-absorption spectroscopy are needed to address the mechanism of network formation and the observed thermodynamic preference. In the meantime, we propose that the preference for two-fold Au-py coordination and the favourable adsorption of **L** molecules on Au(111) drive the observed selectivity for a pure β1-network phase following thermal annealing.

2.3. α-Networks on Au(111)

The minor α-network phase was reproducibly obtained under a broad range of conditions with different molecule dosages, deposition temperatures, and post-thermal annealing regimes. In total, the occurrence of the α-network is as low as 9.2%, in terms of the portion of the molecules in α-network versus the total amount of the molecules ($\approx 6\times10^4$, corresponding to an absolute coverage $\approx 0.5\ \mu m^2$ for β-networks.) By carefully inspecting in large surface areas, we observed frequently that α-networks extended from the lower step edges of the substrate, in an epitaxial growth mode (ellipses in Figure 3a).[19] Unit cell parameters of the α-network (black rhombus in Figure 3b) indicate that $|\boldsymbol{a}| = |\boldsymbol{b}| = 2.17 \pm 0.02$ nm. The deduced projected Au–N bond length was 2.5 ± 0.1 Å, similar to that for α-networks on Ag(111) (2.7 Å), but much larger than that for β-networks (≈1.5–1.6 Å).

Au coordination centres can be supplied by gas adatoms released from kink sites, step edges and other defects.[34] The α-networks on Au(111) were frequently observed in the proximity of the lower step edges, where the density of Au adatoms is much higher than that in open terraces according to the Gibbs-Thomson relationship in two dimensions.[41,42] This suggests that α-networks tend to emerge on Au(111) in areas where the density of Au adatoms is high. In agreement with this tendency, the absolute concentration of Au coordination centres for the α-network (0.245 nm^{-2}) was also higher than that for the β-network (0.216 nm^{-2}). Thereby, we propose that the formation of α-network on Au(111) is predominated by the presence of a high density of Au adatoms in local surface areas.

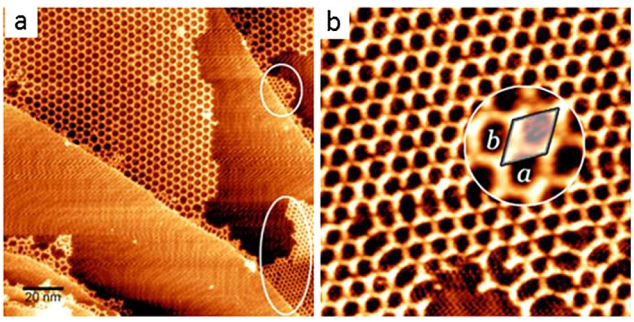

Figure 3. a) Typical STM topograph showing the coexistence of α-networks and β-networks on Au(111). The two ellipses denote α-networks. b) High-resolution image (30 nm×30 nm) of the α-networks on Au(111). The circular inset shows a unit cell with $|\boldsymbol{a}| = |\boldsymbol{b}| = 2.17 \pm 0.02$ nm.

2.4. The α-Network Formation Induced with an STM Tip

Given the distinct bonding modes of Au (ad)atoms on Au(111), we attempted to use an STM tip to locally create α-networks from a homogeneous β1-network phase. We scanned surface areas covered with β1-networks using tunnelling conditions $U = -50$ mV and $I = 80$ pA, as well as an atypical scanning speed (v) ≈50 ms/line, which is three times faster than the normal speed (150–250 ms/line). The typical feedback circuit was retained. These scanning conditions were set so that "tip contact" to the surface,[41–43] and thus the damage of the β1-networks were expected. To further disturb β1-networks beneath the tip and create Au islands,[41] we applied voltage pulses (−2 V, and the time span is ≈30 ms.) randomly during scanning. Afterwards, we rescanned the surface using normal tunnelling conditions ($U = -1.2$ V, $I = 50$ pA, $v = 150$–250 ms/line) and observed small sheets of α-network. These α-networks are visible in Figure 4a, where frame **1** (20 nm×20 nm) denotes the area we manipulated. In the frame, a small Au island, presumably created by a pulse of −2 V, is visible on the right side. Repeat scanning showed that α-network sheets became larger and more stable within 30 min (Figure 4b). The α-networks did not strictly embrace the Au island because of the instability of molecules at the borders of the β1-networks, and of the perturbing of the STM tip. Nevertheless, we propose that the high density of the Au adatoms in the Au island likely helped to drive growth of the α-networks as follows. The STM tip and high-voltage pulses created small islands or craters,[41,42] and the released **L** molecules re-assembled into α-networks, which was driven by the high adatom density maintained by the Au islands. Because of the instability of the tip and the unknown shape of its apex, this approach may cause an unintended "damage" to the networks and the substrate, and therefore the size and the shape of resultant α-networks are somehow less controlled. As the resultant α-networks appeared at open terraces (i.e. with low Au adatom density), we expected that re-annealing would transform them back to β-networks.

In the second approach to locally manipulate the two-dimensional coordination network, we gradually increased the tunnelling setpoint or decreased the magnitude of bias voltages. The STM tip was therefore brought closer to the sample, to gently "disturb" surface structures. This approach simultaneously allowed for surface imaging. Figure 4c shows a typical image obtained during scanning of frame **2** (20 nm×20 nm) with reduction in the magnitude of bias voltages from −1.2 V

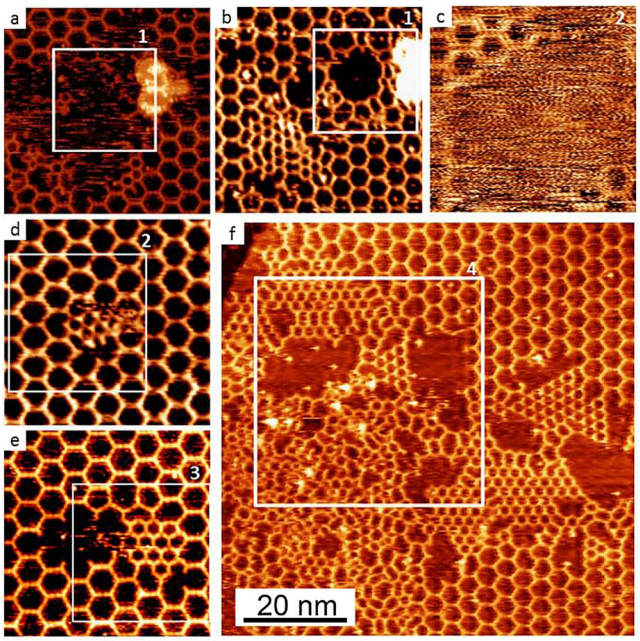

Figure 4. Creation of α-networks within β1-network domains using an STM tip. a) An image obtained after an atypical scanning ($U=-50$ mV, $I=80$ pA; the scanning area is indicated by the white square frame marked by **1**) shows that α-networks appear around the frame. A small Au island, induced by tip pulses, is visible on the right side of the frame. b) α-networks grow and become more stable after 30 min. c) A typical STM image of frame **2**. The image was obtained during an atypical scanning ($U=-1.2$ to -0.05 V, $I=50$ pA). d) α-network appearing in frame **2**. e) α-network emerging after an atypical scanning ($U=+1.2$ V, $I=160$ pA) in frame **3**. f) Large α-network domains. The image was obtained after an atypical scanning ($U=-0.05$ V, $I=160$ pA). The scanning speed (v) for all atypical scan was ≈50 ms/line. Scale: (a, b) 40 nm×40 nm; (c) 20 nm×20 nm; (d, e) 30 nm×30 nm.

to −0.2 V and then to −50 mV; I was kept constant at 50 pA, and v was kept constant at ≈50 ms/line. The "steamy" appearance in the central area suggested that the β1-network had partially dissociated, and that "released" **L** molecules had been migrating on the surface, and thus not resolved by STM. After reshaping the STM tip elsewhere, we rescanned the area and observed a small sheet of α-network in frame **2** (Figure 4d). No Au island, however, was observed. We propose that the high density of Au adatoms necessary for α-network formation arose when Au atoms transferred onto the tip and then back onto the substrate. Such transfer, well known to occur during STM of metallic surfaces,[43] is especially likely under our atypical scanning conditions involving an extremely short tip-sample distance or more frequent "tip-contacts". The α-networks obtained under these experimental conditions were smaller than the scanning frames, suggesting that the density of Au adatoms (i.e. the absolute number of Au adatoms within the scanning area) transferred on the substrate from the tip was not high enough to allow extensive assembly of α-networks (Figure 4d).

In the third approach, we scanned frame **3** (20 nm×20 nm) continuously for 15 min using a positive bias voltage ($U=+1.2$ V, $I=160$ pA, $v\approx50$ ms/line), which generated a small patch of α-network (Figure 4e). We propose that using positive bias voltages one can inject electrons from the tip into molecules, which are thus destabilized by the additional kinetic energy brought by the electrons.[43–46] At the same time, the fast scanning speed causes unintended "tip contacts" to the surface, thereby damaging the β-network and producing Au adatoms. The magnitude of bias voltages per se were found not to be essential for α-network formation, since the bias voltages from −2.0 V to +3.5 V were used and produced similar results. This allows us to exclude electric fields or sample polarity as an essential factor in these local manipulation of the coordination networks.[18]

Using the approaches aforementioned, we were able to create α-network domains as large as ≈25 nm by scanning within larger frames. As shown in Figure 4f, frame **4** (40 nm× 40 nm) was scanned using $U=-50$ mV, $I=160$ pA and $v\approx50$ ms/line. The resulted α-networks extended outside the scanning frame, probably reflecting tip-substrate contacts and the dynamic nature of the self-assembly.

These experiments demonstrate a local manipulation on the polymorphism of coordination networks, where we could locally create α-networks (out of three-fold Au-py coordination) by damaging the β1-network (out of two-fold Au-py coordination) using tip contact during fast STM scanning. Such a process depends on a high density of Au adatoms produced either through Au atom transfer from an STM tip, or through formation of Au islands induced by voltage pulses or "tip-contacts".

3. Conclusions

We have achieved global and local control of two-dimensional Au-pyridyl coordination networks on metal surfaces. Both types of control are determined by the adsorption of organic molecules and the density of Au adatoms. We believe that a similar strategy can be valid for coordination systems involving other labile metal coordination centres such as Fe or Co. Controlling polymorphism of coordination networks at either micro or nanoscale by tailoring the metal coordination motifs may allow for a full manoeuvre over the catalytic and spintronic properties of a functional surface. The local manipulations shown here, performed on a homogeneous single-crystalline β1-network region, may support artificial patterning of a metal-organic functional surface potential for optical/electronic nanodevices.

Experimental Section

Sample preparation processes were performed in an ultrahigh vacuum (UHV) system (SPECS GmbH) at a base pressure ≈3.0×10^{-10} mbar. The single-crystal Ag(111) and Au(111) substrates (MaTeck, 99.999%) were cleaned by cycles of Ar ion sputtering at an energy of 900 eV and annealing at 800 K. The atomic lattices of the samples were determined by STM scanning at room temperature that produced atomic-resolution topographs. Au atoms were evaporated, by using an electron-beam evaporator, from gold wires (Alfa, 99.999%) contained by a Mo crucible. The organic compound **L** (1,3,5-tris[4-(pyridin-4-yl)phenyl]benzene, purity > 96%) was evaporated by organic molecular beam epitaxy (DODECON Nanotechnology GmbH) and the sublimation temperature was 390 °C.

All STM experiments were performed using an Aarhus SPM apparatus controlled by the Nanonis electronics. Topographic data were acquired in constant current mode. Typical scan conditions used to imaging topographs: bias voltages (sample vs. tip) $U = -1.2$ to -0.8 V; tunnelling current $I = 50$–200 pA; feedback loop circuit, P gain = 0.2 nm, time constant = 0.3 ms; image resolution, 512×512 pixels; scanning speed (v) $\approx$150–250 ms/line. Atypical scan conditions used to create α-networks were indicated in figure captions.

Acknowledgements

This work was financially supported by the NSFC (21303113, 21672059, 21561162003) and the Natural Science Foundation of Jiangsu Province (BK20130285). Z. S. thanks the China Postdoctoral Science Foundation (2013M540460) for financial support.

Conflict of interest

The authors declare no conflict of interest.

Keywords: coordination networks · global and local control · scanning tunnelling microscopy · self-assembly · surface chemistry

[1] J.-M. Lehn, *Angew. Chem. Int. Ed.* **2013**, *52*, 2836 – 2850; *Angew. Chem.* **2013**, *125*, 2906 – 2921.
[2] S. De Feyter, F. C. De Schryver, *Chem. Soc. Rev.* **2003**, *32*, 139 – 150.
[3] J. V. Barth, G. Costantini, K. Kern, *Nature* **2005**, *437*, 671 – 679.
[4] S. De Feyter, F. C. De Schryver, *J. Phys. Chem. B* **2005**, *109*, 4290 – 4302.
[5] J. V. Barth, *Annu. Rev. Phys. Chem.* **2007**, *58*, 375 – 407.
[6] N. Lin, S. Stepanow, M. Ruben, J. V. Barth, *Top. Curr. Chem.* **2008**, *287*, 1 – 44.
[7] J. V. Barth, *Surf. Sci.* **2009**, *603*, 1533 – 1541.
[8] J. A. A. W. Elemans, S. Lei, S. De Feyter, *Angew. Chem. Int. Ed.* **2009**, *48*, 7298 – 7332; *Angew. Chem.* **2009**, *121*, 7434 – 7469.
[9] L. Bartels, *Nat. Chem.* **2010**, *2*, 87 – 95.
[10] K. Ariga, M. V. Lee, T. Mori, X.-Y. Yu, J. P. Hill, *Adv.Colloid Interface Sci.* **2010**, *154*, 20.
[11] R. Otero, J. M. Gallego, A. L. V. de Parga, N. Martín, R. Miranda, *Adv. Mater.* **2011**, *23*, 5148 – 5176.
[12] Y.-T. Shen, K. Deng, X.-M. Zhang, W. Feng, Q.-D. Zeng, C. Wang, J. R. Gong, *Nano Lett.* **2011**, *11*, 3245 – 3250.
[13] B. E. Hirsch, K. P. McDonald, B. Qiao, A. H. Flood, S. L. Tait, *ACS Nano* **2014**, *8*, 10858 – 10869.
[14] L. Piot, R. M. Meudtner, T. El Malah, S. Hecht, P. Samorì, *Chem. Eur. J.* **2009**, *15*, 4788 – 4792.
[15] M. O. Blunt, J. Adisoejoso, K. Tahara, K. Katayama, M. Van der Auweraer, Y. Tobe, S. De Feyter, *J. Am. Chem. Soc.* **2013**, *135*, 12068 – 12075.
[16] S.-L. Lee, Y. Fang, G. Velpula, F. P. Cometto, M. Lingenfelder, K. Müllen, K. S. Mali, S. De Feyter, *ACS Nano* **2015**, *9*, 11608 – 11617.
[17] T. Sirtl, S. Schlögl, A. Rastgoo-Lahrood, J. Jelic, S. Neogi, M. Schmittel, W. M. Heckl, K. Reuter, M. Lackinger, *J. Am. Chem. Soc.* **2013**, *135*, 691 – 695.
[18] F. P. Cometto, K. Kern, M. Lingenfelder, *ACS Nano* **2015**, *9*, 5544 – 5550.
[19] M. Pivetta, G. E. Pacchioni, E. Fernandes, H. Brune, *J. Chem. Phys.* **2015**, *142*, 101928.
[20] S. Kitagawa, R. Kitaura, S.-i. Noro, *Angew. Chem. Int. Ed.* **2004**, *43*, 2334 – 2375; *Angew. Chem.* **2004**, *116*, 2388 – 2430.
[21] O. M. Yaghi, M. O'Keeffe, N. W. Ockwig, H. K. Chae, M. Eddaoudi, J. Kim, *Nature* **2003**, *423*, 705 – 714.
[22] B. H. Northrop, Y.-R. Zheng, K.-W. Chi, P. J. Stang, *Acc. Chem. Res.* **2009**, *42*, 1554 – 1563.
[23] L. Dong, Z. A. Gao, N. Lin, *Prog. Surf. Sci.* **2016**, *91*, 101 – 135.
[24] W. Xu, J.-g. Wang, M. Yu, E. Lægsgaard, I. Stensgaard, T. R. Linderoth, B. Hammer, C. Wang, F. Besenbacher, *J. Am. Chem. Soc.* **2010**, *132*, 15927 – 15929.
[25] C. Wäckerlin, C. Iacovita, D. Chylarecka, P. Fesser, T. A. Jung, N. Ballav, *Chem. Commun.* **2011**, *47*, 9146 – 9148.
[26] N. Abdurakhmanova, A. Floris, T.-C. Tseng, A. Comisso, S. Stepanow, A. De Vita, K. Kern, *Nat. Commun.* **2012**, *3*, 940.
[27] D. Skomski, S. Abb, S. L. Tait, *J. Am. Chem. Soc.* **2012**, *134*, 14165 – 14171.
[28] T. K. Shimizu, J. Jung, H. Imada, Y. Kim, *Angew. Chem. Int. Ed.* **2014**, *53*, 13729 – 13733; *Angew. Chem.* **2014**, *126*, 13949 – 13953.
[29] C. Zhang, L. Wang, L. Xie, H. Kong, Q. Tan, L. Cai, Q. Sun, W. Xu, *ChemPhysChem* **2015**, *16*, 2099 – 2105.
[30] D. Skomski, C. D. Tempas, B. J. Cook, A. V. Polezhaev, K. A. Smith, K. G. Caulton, S. L. Tait, *J. Am. Chem. Soc.* **2015**, *137*, 7898 – 7902.
[31] D. Écija, J. I. Urgel, A. C. Papageorgiou, S. Joshi, W. Auwärter, A. P. Seitsonen, S. Klyatskaya, M. Ruben, S. Fischer, S. Vijayaraghavan, *Proc. Natl. Acad. Sci. USA* **2013**, *110*, 6678 – 6681.
[32] J. I. Urgel, D. Écija, W. Auwärter, J. V. Barth, *Nano Lett.* **2014**, *14*, 1369 – 1373.
[33] G. Lyu, Q. Zhang, J. I. Urgel, G. Kuang, W. Auwärter, D. Écija, J. V. Barth, N. Lin, *Chem. Commun.* **2016**, *52*, 1618 – 1621.
[34] N. Lin, D. Payer, A. Dmitriev, T. Strunskus, C. Wöll, J. V. Barth, K. Kern, *Angew. Chem. Int. Ed.* **2005**, *44*, 1488 – 1491; *Angew. Chem.* **2005**, *117*, 1512 – 1515.
[35] Z. Shi, N. Lin, *J. Am. Chem. Soc.* **2009**, *131*, 5376 – 5377.
[36] J. Meyer, A. Nickel, R. Ohmann, Lokamani, C. Toher, D. A. Ryndyk, Y. Garmshausen, S. Hecht, F. Moresco, G. Cuniberti, *Chem. Commun.* **2015**, *51*, 12621 – 12624.
[37] M. Matena, J. Björk, M. Wahl, T.-L. Lee, J. Zegenhagen, L. H. Gade, T. A. Jung, M. Persson, M. Stöhr, *Phys. Rev. B* **2014**, *90*, 125408.
[38] P. Maksymovych, J. T. Yates, *J. Am. Chem. Soc.* **2008**, *130*, 7518 – 7519.
[39] S. Gottardi, K. Müller, J. C. Moreno-López, H. Yildirim, U. Meinhardt, M. Kivala, A. Kara, M. Stöhr, *Adv. Mater. Interfaces* **2014**, *1*, 1300025.
[40] D. Kühne, F. Klappenberger, R. Decker, U. Schlickum, H. Brune, S. Klyatskaya, M. Ruben, J. V. Barth, *J. Am. Chem. Soc.* **2009**, *131*, 3881 – 3883.
[41] R. C. Jaklevic, L. Elie, *Phys. Rev. Lett.* **1988**, *60*, 120 – 123.
[42] K. Morgenstern, G. Rosenfeld, G. Comsa, *Phys. Rev. Lett.* **1996**, *76*, 2113 – 2116.
[43] C. Bai, in *Scanning Tunneling Microscopy and Its Applications, Vol. 32*, Springer, Berlin, New York, **2000**.
[44] S.-W. Hla, L. Bartels, G. Meyer, K.-H. Rieder, *Phys. Rev. Lett.* **2000**, *85*, 2777 – 2780.
[45] J. Liu, C. Li, X. Liu, Y. Lu, F. Xiang, X. Qiao, Y. Cai, Z. Wang, S. Liu, L. Wang, *ACS Nano* **2014**, *8*, 12734 – 12740.
[46] H. Kong, L. Wang, Q. Sun, C. Zhang, Q. Tan, W. Xu, *Angew. Chem. Int. Ed.* **2015**, *54*, 6526 – 6530; *Angew. Chem.* **2015**, *127*, 6626 – 6630.

Manuscript received: April 24, 2017
Accepted manuscript online: May 17, 2017
Version of record online: June 7, 2017